Medicinal Chemistry Research (2019) 28:465–472
https://doi.org/10.1007/s00044-019-02299-4

MEDICINAL CHEMISTRY RESEARCH

ORIGINAL RESEARCH

Design, synthesis and anticancer activities of halogenated Phenstatin analogs as microtubule destabilizing agent

Shengquan Hu[1] · Wuji Sun[1] · Yeming Wang[2] · Hong Yan[1]

Received: 30 November 2018 / Accepted: 24 January 2019 / Published online: 4 February 2019

Abstract

A series of halogenated Phenstatin analogs were designed as microtubule destabilizing agent by docking study. It was synthesized within three steps starting from 2-chloro-5-iodobenzoic acid and substituted benzene. All the products were characterized by ^{1}H NMR and ^{13}C NMR spectral analysis, and the stereochemical structure was also confirmed by a single crystal X-ray diffraction crystallographic analysis. The microtubule destabilizing activities were evaluated in vitro with human liver cancer Huh-7 cell line and human lung cancer A549 cell line. Some of the HPAs were achieved IC_{50} about 5.0 μM against human liver cancer Huh-7 cells.

Graphical Abstract

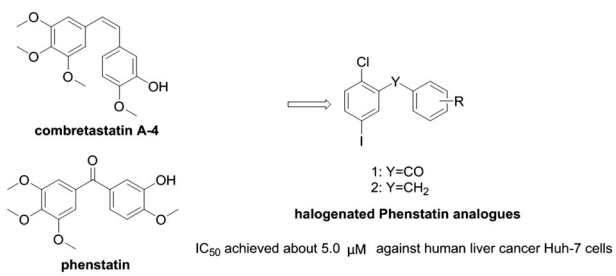

Keywords Phenstatin analogs · Microtubule destabilizing agent · Docking · Anticancer · CCK-8

Introduction

Combretastatins are natural antimitotic stilbenes derived from the bark of Combretum caffrum Kuntze (Combretaceae) (Pettit et al. 1982). The three most active molecules Combretastatin A-1, A-2, and A-4 (CA-4) (Fig. 1) have attracted a great attention as potent inhibitors of tubulin polymerization (Lin et al. 1989; Pettit et al. 2003; Kingston 2009). Combretastatins have special characteristics that they can selectively target on the tumor blood vessels and destroy the central area of the tumor (Li and Tian 2016). Moreover, the CA-4 class of microtubule destabilizing agent cannot be recognized by the drug efflux transporter P-glycoprotein, which excessive expression in tumor cells results in drug resistance (Singh and Kaur 2009). However, clinical studies have found that Combretastatins have elevated blood pressure and other cardiovascular toxicities (Li and Tian 2016). Optimization structure of lead compounds Combretastatins and synthesis of new type Combretastatins derivatives with more efficient and lower toxicity appear to be very important.

The reported structural modifications of Combretastatins have focused on trisubstituted benzene rings and double

✉ Hong Yan
hongyan@bjut.edu.cn

[1] Beijing Key Laboratory of Environmental and Viral Oncology, College of Life Science and Bio-engineering, Beijing University of Technology, Beijing, China

[2] Beijing Tide Pharmaceutical Co., Ltd, Beijing, China

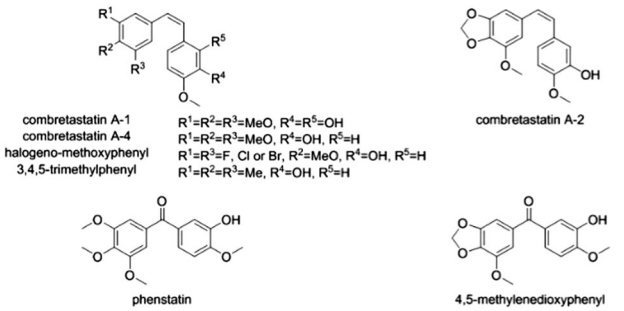

Fig. 1 Microtubule destabilizing agent structures

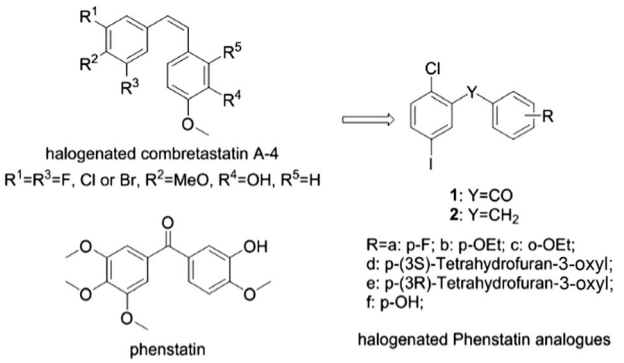

Scheme 1 Design strategy of HPAs

bond linker. The trisubstituted of CA-4, such as 2,3,4-trimethoxyphenyl (Álvarez et al. 2010), halogeno-methoxyphenyl (Beale et al. 2010), and 3,4,5-trimethylphenyl (Gaukroger et al. 2003) moieties, were demonstrated equal or better activity. The pharmacophore model indicates that other hydrogen bond acceptors could replace the trimethoxy group (Fig. 1) (Marrelli et al. 2011; Nguyen et al. 2005). The replacement of meta-methoxy groups with halogen atoms (F, Cl, or Br) resulted in little difference in growth inhibition of human cancer cell line comparison to CA-4 (Pettit et al. 2005). Phenstatin (Fig. 1) was designed from the CA-4 skeleton by replacement of the double bond linker with a carbonyl moiety (Pettit et al. 1998). It is a potent microtubule destabilizing agent that interacts with colchicine binding site of tubulin and displays significant anticancer and antimitotic activities comparable to those of CA-4 (Pettit et al. 1998; 2000). 4,5-methylenedioxyphenyl analog displaying the antiproliferative tubulin-destabilizing activity at the same concentration range as CA-2 and CA-4 (Titov et al. 2011). A halogenated Phenstatin analogs (HPAs), as an intermediate of Empagliflozin, was attracted much attention for the very similar structure to that of some reported microtubule destabilizing agents (Wang et al. 2014).

In order to better study tubulin polymerization inhibition of Phenstatin analogs, HPAs were designed based on the importance of halogen in the Combretastatin (Scheme 1). The activities of the HPAs (**1** and **2**) were evaluated according to their binding energy (ΔG) and inhib constant (Ki) by the virtual screening on Auto-Dock 4.0. The synthesis of HPAs and anticancer activities evaluation were described in details.

Materials and methods

Theoretical calculation

Initially, the virtual screening was utilized to identify the potential inhibition of HPAs on tubulin polymerization. The Tubulin-CA4 complex (PDB ID: 5lyj) (Gaspari et al. 2017) was chosen as the study targets, owing to the ligand CA-4 is similar structure to HPAs.

Molecular docking of compounds into the Tubulin-Combretastatin A4 complex (PDB ID: 5lyj) was carried out using the AutoDock software package as implemented through the graphical user interface AutoDockTools (ADT 1.5.2). ADT was used to add polar hydrogens and gasteiger charges. Ligands were prepared by drawing the 2D structure in ChemDraw, and converted to PDB format using Chem3D. Ligands were then energy minimized using Discovery Studio Visualizer before using ADT to add polar hydrogens and gasteiger charges. All bound water and ligands were eliminated from the protein and the polar hydrogen was added. The whole Tubulin-Combretastatin A4 complex was defined as a receptor and the site sphere was selected based on the ligand binding location of Original ligand, then the molecule of Original ligand CA-4 was removed and new ligand was placed during the molecular docking procedure. Types of interactions of the docked protein with ligand were analyzed after the end of molecular docking.

Materials and compound synthesis

Chemical reagents and solvents were obtained from commercial sources. Commercial grade reagents were used without further purification. When necessary, solvents were dried or purified by standard methods. Melting points (m.p.) were determined with an Electrothermal 9100 capillary melting point apparatus and are uncorrected. ^{1}H NMR and ^{13}C NMR spectra were obtained using a Bruker 400 Ultrashield^{TM} spectrometer at 400 and 100 MHz respectively. These were analyzed using the Bruker TOPSPIN 2.1 program. Chemical shifts are reported in parts per million relative to internal tetramethylsilane standard. Coupling constants (J) are quoted to the nearest 0.1 Hz. The following abbreviations are used: s, singlet; d, doublet; t, triplet; q, quartet; m, multiplet and br, broad. High resolution mass spectra (HRMS) were obtained on a Thermo LTQ Orbitrap

XL (ThermoFisher, San Jose, CA, USA) spectrometer, equipped with a quantropole detector. Analytic thin-layer chromatography (TLC) was performed on the glass-backed silica gel sheets (silica gel GF254). All compounds were detected using UV light (254 or 365 nm).

General procedure for the synthesis of HPAs (1a–1e)

To a stirred suspension of 2-chloro-5-iodobenzoic acid (5.65 g, 0.02 mol) in CH_2Cl_2(20 mL) was added oxalyl chloride(1.80 mL, 0.021 mol) and DMF(0.02 mL). The resulting mixture was stirred for 4 h at room temperature. The mixture was concentrated, and the residual colorless solid was dissolved in CH_2Cl_2(40 mL). To this solution were added corresponding substituted benzene(0.02 mol) and then $AlCl_3$(2.75 g, 0.021 mol) portionwise so that the temperature did not exceed 0 °C. After being stirred at 10–20 °C for 3 h, the mixture was poured into ice water and extracted with CH_2Cl_2 three times. The combined organic layers were washed with 1 M HCl, water, and brine, then dried over $MgSO_4$ and concentrated. The residual solid was crystallized from ethanol to give as white solid.

According to this procedure the following compounds were prepared.

(2-chloro-5-iodophenyl)(4-fluorophenyl)methanone (1a)

White solid, yield 92%, m.p. 69–70 °C. ^{1}H NMR (400 MHz, DMSO-d_6): δ 7.38–7.40(m, 2H), 7.41(d, J = 8.0 Hz, 1H), 7.82 (dd, J = 2.4 Hz, 8.0 Hz, 2H), 7.90(d, J = 2.4 Hz, 1H), 7.92–7.95(m, 1H). ^{13}C NMR (100 MHz, DMSO-d_6): δ 116.19, 129.47, 131.65, 132.1, 132.65, 136.78, 139.69, 140.20, 164.54, 166.56, 191.36. HRMS (ESI) *m/z* (pos):382.91890 $C_{13}H_7ClFIONa$ $[M + Na]^+$(calcd. 382.91118).

(2-chloro-5-iodophenyl)(4-ethoxyphenyl)methanone (1b)

White solid, yield 72%, m.p. 103–104 °C. ^{1}H NMR (400 MHz, DMSO-d_6): δ 1.36(t, J = 5.6 Hz, 3H), 4.14(q, J = 5.6 Hz, 2H), 7.06(d, J = 6.8 Hz, 2H), 7.38(d, J = 6.8 Hz, 1H), 7.69(d, J = 6.8 Hz, 2H), 7.82(d, J = 0.8 Hz, 1H), 7.90(dd, J = 0.8, 6.8 Hz, 1H). ^{13}C NMR (100 MHz, DMSO-d_6): δ 14.31, 63.69, 92.74, 114.64, 128.04, 129.45, 131.54, 132.05, 136.53, 139.72, 140.43, 163.31, 191.03. HRMS (ESI) *m/z* (pos):386.96463 $C_{15}H_{13}ClIO_2$ $[M+H]^+$(calcd. 386.96488).

(2-chloro-5-iodophenyl)(2-ethoxyphenyl)methanone (1c)

White solid, yield 18%, m.p. 109–110 °C. ^{1}H NMR (400 MHz, DMSO-d_6): δ 0.81(t, J = 5.6 Hz,3H), 3.85(q, J = 5.6 Hz, 2H), 7.08–7.12(m, 2H), 7.30(d, J = 6.8 Hz, 1H), 7.59–7.63(m, 1H), 7.66(d, J = 0.8 Hz, 1H), 7.72(dd, J = 0.8, 6.8 Hz, 1H), 7.83(dd, J = 0.8, 6.8 Hz, 1H). ^{13}C NMR (100 MHz, DMSO-d_6): δ 13.58, 63.54, 92.07, 113.23, 120.67, 125.82, 129.30, 130.42, 131.31, 135.39, 136.20, 139.29, 143.17, 158.36, 192.09. HRMS (ESI) *m/z* (pos):386.96463 $C_{15}H_{13}ClIO_2$ $[M+H]^+$(calcd. 386.96488).

(*S*)-(2-chloro-5-iodophenyl)(4-((tetrahydrofuran-3-yl)oxy) phenyl)methanone (1d)

White solid, yield 81%, m.p. 110–111 °C. ^{1}H NMR (400 MHz, DMSO-d_6): δ 1.96–2.00(m, 1H), 2.24–2.31(m, 1H), 3.74–3.78(m, 1H), 3.81–3.88(m, 2H), 3.90–3.93(m, 1H), 5.14–5.16(m, 1H), 7.06(d, J = 6.8 Hz, 2H), 7.38(d, J = 6.8 Hz, 1H), 7.69(d, J = 6.8 Hz, 2H), 7.82(d, J = 0.8 Hz, 1H), 7.90(dd, J = 0.8, 6.8 Hz, 1H). ^{13}C NMR (100 MHz, DMSO-d_6): δ 32.36, 66.35, 72.11, 77.79, 92.82, 115.46, 128.24, 129.43, 131.58, 132.11, 136.55, 139.79, 140.38, 162.00, 191.10. HRMS (ESI) *m/z* (pos):428.97536 $C_{17}H_{15}ClIO_3$ $[M+H]^+$(calcd. 428.97544).

(*R*)-(2-chloro-5-iodophenyl)(4-((tetrahydrofuran-3-yl)oxy) phenyl)methanone (1e)

White solid, yield 83%, m.p. 108–110 °C. ^{1}H NMR (400 MHz, DMSO-d_6): δ 1.96–1.99(m, 1H), 2.25–2.99(m, 1H), 3.74–3.80(m, 1H), 3.80–3.88(m, 2H), 3.90–3.93(m, 1H), 5.14–5.16(m, 1H), 7.06(d, J = 6.8 Hz, 2H), 7.38(d, J = 6.8 Hz, 1H), 7.69(d, J = 6.8 Hz, 2H), 7.82(d, J = 0.8 Hz, 1H), 7.90(dd, J = 0.8, 6.8 Hz, 1H). ^{13}C NMR (100 MHz, DMSO-d_6): δ 32.36, 66.35, 72.12, 77.80, 92.85, 115.48, 128.25, 129.42, 131.59, 132.12, 136.55, 139.81, 140.39, 162.02, 191.12. HRMS (ESI) *m/z* (pos):428.97536 $C_{17}H_{15}ClIO_3$ $[M+H]^+$(calcd. 428.97544)

Procedure for the synthesis of halogenated Phenstatin analog (2-chloro-5-iodophenyl)(4-hydroxyphenyl) methanone (1f)

To a solution of **1b** (5.79 g, 0.015 mmol) in dichloromethane(60 mL) at −20 °C was added boron tribromide (1.65 mL, 0.023 mol) over 10 min at a rate that maintained the reaction temperature below −10 °C under argon. After addition, the mixture was slowly warmed to 0 °C and stirred for 3 h. The reaction mixture was poured into 100 mL of ice water and extracted with dichloromethane(2 × 100 mL). The combined organic layers were washed with saturated bicarbonate(80 mL), water(80 mL), and brine(80 mL) and then dried over Na_2SO_4. The sample was concentrated and purified by silica gel column chromatography to give product **1f** as a white solid, yield 87%, m.p. 181–182 °C. ^{1}H NMR (400 MHz, DMSO-d_6): δ 6.88(d, J = 6.8 Hz, 2H), 7.37(d, J = 6.8 Hz, 1H), 7.58(d, J = 6.8 Hz, 2H), 7.78(d, J = 0.8 Hz, 1H), 7.88(dd, J = 0.8, 6.8 Hz, 1H), 10.64(s, 1H).

^{13}C NMR (100 MHz, DMSO-d_6): δ 115.70, 126.84, 129.44, 131.54, 132.40, 136.48, 139.59, 140.74, 163.20, 190.88. HRMS (ESI) *m/z* (pos):356.91777 $C_{13}H_7ClIO_2$ $[M-H]^-$(calcd. 356.91793)

General procedure for the synthesis of HPAs (2)

To a stirred solution of **1** (0.01 mol) in 30 mL of CH_2Cl_2 and 30 mL of CH_3CN at 0 °C were added Et_3SiH(4.79 mL, 0.03 mol), then $BF_3{\cdot}Et_2O$(2.53 mL, 0.02 mol), and the resulting mixture was warmed to room temperature and stirred for 3–8 h. The mixture was poured into saturated aqueous $NaHCO_3$ and extracted with CH_2Cl_2 twice. The combined organic layers were washed with brine, dried over $MgSO_4$, and concentrated. The residual solid was crystallized from ethanol to give as white solid.

According to this procedure the following compounds were prepared.

1-chloro-2-(4-fluorobenzyl)-4-iodobenzene (2a)

White solid, yield 83%, m.p. 52–54 °C. ^{1}H NMR (400 MHz, DMSO-d_6): δ 4.02(s, 2H), 7.10–7.13(m, 2H), 7.22–7.25(m, 3H), 7.60(dd, $J = 0.8$, 6.8 Hz, 1H), 7.72(d, $J = 0.8$ Hz, 1H). ^{13}C NMR (100 MHz, DMSO-d_6): δ 36.94, 92.85, 115.21(d, $J = 68$ Hz), 130.30(d, $J = 24$ Hz), 131.32, 133.16, 134.87, 136.82, 139.44, 140.77, 159.80, 161.73.

1-chloro-2-(4-ethoxybenzyl)-4-iodobenzene (2b)

White solid, yield 87%, m.p. 61–63 °C. ^{1}H NMR (400 MHz, DMSO-d_6): δ 1.30(t, $J = 5.6$ Hz, 3H), 3.94(s, 2H), 3.97(q, $J = 5.6$ Hz, 2H), 6.84(d, $J = 5.6$ Hz, 2H), 7.09(d, $J = 5.6$ Hz, 2H), 7.22(d, $J = 6.8$ Hz, 1H), 7.58(dd, $J = 0.8$, 6.8 Hz, 1H), 7.65(d, $J = 0.8$ Hz, 1H). ^{13}C NMR (100 MHz, DMSO-d_6): δ 14.57, 36.95, 62.83, 92.76, 114.36, 129.59, 130.44, 131.25, 133.08, 136.57, 139.31, 141.41, 156.99.

1-chloro-2-(2-ethoxybenzyl)-4-iodobenzene (2c)

White solid, yield 81%, m.p. 73–75 °C. ^{1}H NMR (400 MHz, DMSO-d_6): δ 1.30(t, $J = 5.6$ Hz, 3H), 3.95(s, 2H), 4.00(q, $J = 5.6$ Hz, 2H), 6.85–6.88(m, 1H), 6.95–6.97(m, 1H), 7.05–7.07(m, 1H), 7.19–7.23(m, 2H), 7.55–7.57(m, 2H). ^{13}C NMR (100 MHz, DMSO-d_6): δ 14.54, 63.08, 92.36, 111.63, 120.12, 126.41, 127.96, 130.12, 131.05, 133.30, 136.33, 139.50, 140.39, 156.24.

(*S*)-3-(4-(2-chloro-5-iodobenzyl)phenoxy)tetrahydrofuran (2d)

White solid, yield 79%, m.p. 60–62 °C. ^{1}H NMR (400 MHz, DMSO-d_6): δ 1.92–1.95(m, 1H), 2.15–2.19(m, 1H), 3.71–3.77(m, 2H), 3.81–3.85(m,1H), 3.95(s, 2H), 4.93–4.96(m, 1H), 6.84(d, $J = 5.6$ Hz, 2H), 7.10(d, $J = 5.6$ Hz, 2H), 7.22(d, $J = 6.8$ Hz, 1H), 7.58(dd, $J = 0.8$, 6.8 Hz, 1H), 7.65(d, $J = 0.8$ Hz, 1H). ^{13}C NMR (100 MHz, DMSO-d_6): δ 32.37, 36.94, 66.29, 72.18, 76.89,92.73, 115.20, 129.66, 130.76, 131.21, 133.10, 136.57, 139.31, 141.27, 155.57.

(*R*)-3-(4-(2-chloro-5-iodobenzyl)phenoxy)tetrahydrofuran (2e)

White solid, yield 74%, m.p. 58–60 °C. ^{1}H NMR (400 MHz, DMSO-d_6): δ 1.90–1.95(m, 1H), 2.14–2.20(m, 1H), 3.70–3.76(m, 2H), 3.78–3.88(m, 2H), 3.94 (s, 2H), 4.94–4.95 (m, 1H), 6.83(d, $J = 6.8$ Hz, 2H), 7.10(d, $J = 6.8$ Hz, 2H), 7.20(d, $J = 6.8$ Hz, 1H), 7.56(dd, $J = 0.8$, 6.8 Hz, 1H), 7.67(d, $J = 0.8$ Hz, 1H) ^{13}C NMR (100 MHz, DMSO-d_6): δ 32.37, 36.93, 66.30, 72.19, 76.91, 92.76, 115.22, 129.67, 130.78, 131.24, 133.10, 136.59, 139.33, 141.29, 155.59.

4-(2-chloro-5-iodobenzyl)phenol (2f)

White solid, yield 75%, m.p. 101–102 °C. ^{1}H NMR (400 MHz, DMSO-d_6): δ 3.90(s, 2H), 6.68(d, $J = 5.6$ Hz, 2H), 6.98(d, $J = 5.6$ Hz, 2H), 7.22(d, $J = 6.8$ Hz, 1H), 7.58(dd, $J = 0.8$, 6.8 Hz, 1H), 7.62(d, $J = 0.8$ Hz, 1H), 9.22(s, 1H). ^{13}C NMR (100 MHz, DMSO-d_6): δ 37.01, 92.75, 115.24, 128.75, 129.57, 131.23, 133.06, 136.49, 139.27, 141.65, 155.76. HRMS (ESI) *m/z* (pos):342.93842 $C_{13}H_9ClIO$ $[M-H]^-$(calcd. 342.93866)

X-ray crystal of compound (1d)

To unambiguously assign the stereochemical structure of compound **1d**, a single crystal X-ray diffraction study was performed. After many attempts, X-ray quality compound **1d** crystals were obtained by slow evaporation of ethanol at room temperature. The X-ray crystal structure of compound **1d** confirmed the stereochemical assignment. And crystallographic data for **1d** has been deposited with Cambridge Crystallographic Data Centre as supplementary number CCDC 1444717. Copies of the data can be obtained, free of charge, on application to CCDC, 12 Union Road, Cambridge CB2 1EZ, UK.

Cytotoxicity assay

For the evaluation of cytotoxicity, two different cancer cell lines were used: human liver cancer Huh-7 cell line and human lung cancer A549 cell line. Cancer cells were cultured according to the supplier's instructions. Cells were seeded in 96-well plates at a density of 2–4 × 10^4 cells per well and incubated overnight in 0.1 mL of media supplemented with 10 % Fetal Bovine Serum (Hyclone, USA) in a

Table 1 Docking results of HPAs

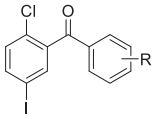

Compound	R group	Binding energy ΔG (kcal/mol)	Inhib constant Ki (μM)
1a	*p*-F	−6.28	24.86
1b	*p*-OEt	−6.11	33.28
1c	*o*-OEt	−6.08	34.88
1d	*p*-(3 S)-Tetrahydrofuran-3-oxyl	−7.47	3.32
1e	*p*-(3 R)-Tetrahydrofuran-3-oxyl	−7.52	3.08
1f	*p*-OH	−6.61	14.36
2a	*p*-F	−6.17	29.78
2b	*p*-OEt	−6.01	39.00
2c	*o*-OEt	−6.00	39.77
2d	*p*-(3 S)-Tetrahydrofuran-3-oxyl	−7.21	5.15
2e	*p*-(3 R)-Tetrahydrofuran-3-oxyl	−7.48	3.30
2f	*p*-OH	−6.35	21.97
CA-4	—	−5.17	163.46
Phenstatin	—	−4.83	286.46

5% CO_2 incubator at 37 °C. On day 2, culture medium in each well was exchanged with 0.1 mL aliquots of medium containing graded concentrations of compounds. On day 4, 5 μL of the cell counting kit-8 solution (Dojindo, Japan) was added to each well and then incubated for additional 4 h under the same conditions. The absorbance of each well was determined by an Automatic Elisa Reader System (Bio-Rad 3550) at a 450 nm wavelength. For determination of the IC_{50} values, the absorbance readings at 450 nm were fitted to the four-parameter logistic equation. Vincristine was purchased from Sigma and used as a positive control.

Results and discussion

Docking studies

The virtual screening results (Table 1) indicated that all the values of binding energy ΔG are between −6.00 and −7.52 kcal/mol; the values of inhib constant Ki are from 3.08 to 39.77 μM. The binding energy value of the original ligand molecule CA-4 and Phenstatin are −5.17 and −4.83 kcal/mol, respectively and the inhib constant are 163.46 and 286.46 μM, respectively. All the values of HPAs are better than that of CA-4 or Phenstatin which reveal potential value for further research.

The screening results also revealed that all the HPAs can conformational adapt to colchicine site appropriately as same as the reported binding mode reported by Gaspari et al. (Gaspari et al., 2017). All the HPAs buried in a hydrophobic pocket shaped by residues CYS241, LEU242, LEU248, ALA250, LEU255, ALA316, ALA354, ASN258, LYS352, VAL181, MET259, VAL315, and ASN350. Table 2 gives the interaction relationship between compounds and amino acid residues. 'A' indicates that the amino acid residue interacts with a halogen-substituted ring; 'B' indicates that the amino acid residue interacts with a non-halogen substituted ring; 'O' indicates that the amino acid residue interacts with a carbonyl group; '-' indicates that the amino acid residue does not interact with the compound.

The superimpositions of HPAs onto original ligand CA-4 in colchicine site of tubulin have shown that there were two kinds of binding mode (Fig. 2). Compounds **1a, 1c, 2a, 2b, 2c**, and **2f** perform the same binding mode (mode HT) which the halogenated benzene ring pile on the 3′-hydroxy-4′-methoxy-substituted B ring of CA-4 (Fig. 2a); On the other hand, the binding mode (mode HH) of compounds **1b, 1d, 1e, 1f, 2d** and **2e** in contrast, which the halogenated benzene ring pile on the 3,4,5-methoxy-substituted A ring of CA-4 (Fig. 2b).

Chemistry

Compounds **1a**–**1f** and **2a**–**2f** were successfully synthesized within three-step reaction starting from 2-chloro-5-iodobenzoic acid and substituted benzene (Scheme 2). Commercially 2-chloro-5-iodobenzoic acid was converted to the corresponding benzoyl chlorides with oxalyl chloride and under Friedel-Crafts conditions. The acylation with phenyl group generated a mixture of regioisomers of diarylketone **1** in favor of the desired *p*-benzophenone purified by recrystallization from ethanol. The reduction of diarylketone **1** by triethylsilane in the presence of boron trifluoride etherate provided **2** in good yield. Compound **1f** was generated via deethylation from **1b** with boron tribromide in 87% yield. It is worth mentioning that *o*-benzophenone **1c** (R = *o*-OEt) was successfully separated and purified.

In this study, all the products were isolated as white solids and characterized by ^{1}H NMR and ^{13}C NMR spectral analysis. To unambiguously assign the stereochemical structure of product, **1d** was performed single crystal X-ray diffraction study. The X-ray diffraction crystallographic analysis of product **1d** confirmed the stereochemical structure assignment (Fig. 3). And crystallographic data for **1d** has been deposited with Cambridge Crystallographic Data Centre as supplementary number CCDC 1444717.

Table 2 Interaction relationship between HPAs and amino acid residues

	1a	1b	1c	1d	1e	1f	2a	2b	2c	2d	2e	2f	CA-4[a]
VAL238	–	–	–	–	–	–	–	–	–	–	–	–	Ar
CYS241	B	A	B	A	A	A	B	B	B	A	A	B	Ar
LEU242	–	A	–	A	A	A	–	–	–	A	A	–	Ar
LEU248	AB	A	AB	A	–	AB	AB	AB	AB	A	–	AB	Ar
ALA250	–	A	B	A	A	AB	–	B	–	A	A	–	Ar
LEU255	O	A	BO	A	AB	AO	–	B	B	AB	AB	–	Ar
ALA316	AB	AB	AB	AB	AB	A	AB	B	AB	AB	AB	AB	Ar
ILE318	–	–	–	–	A	–	–	B	–	–	A	–	Ar
ALA354	B	A	B	A	A	–	B	–	B	A	A	B	Ar
ILE378	–	–	–	–	–	–	–	–	–	–	–	–	Ar
ASN258	–	B	–	B	B	O	–	–	–	B	B	–	Br
LYS352	AB	AB	AB	AB	B	A	AB	AB	AB	AB	B	AB	Br
THR179	–	–	–	–	–	–	–	–	–	–	–	–	Br
ALA180	–	–	–	–	–	–	–	–	–	–	–	–	Br
VAL181	–	B	–	B	B	–	A	A	A	B	B	–	Br
MET259	A	B	A	B	B	–	A	A	A	B	B	A	Br
ASN349	–	–	–	B	–	–	–	–	–	B	–	–	Br
ALA317	B	–	–	–	–	–	B	B	–	–	–	B	–
VAL315	–	B	–	B	B	–	–	–	–	B	B	–	–
ASN350	–	–	–	B	B	–	A	A	A	–	–	A	–
LYS254	–	–	–	–	–	B	–	–	–	–	–	–	–

[a]Ar indicates that the amino acid residue interacts with 3,4,5-methoxy-substituted A ring; Br indicates that the amino acid residue interacts with 3′-hydroxy-4′-methoxy-substituted B ring reported by Gaspari et al. 2017

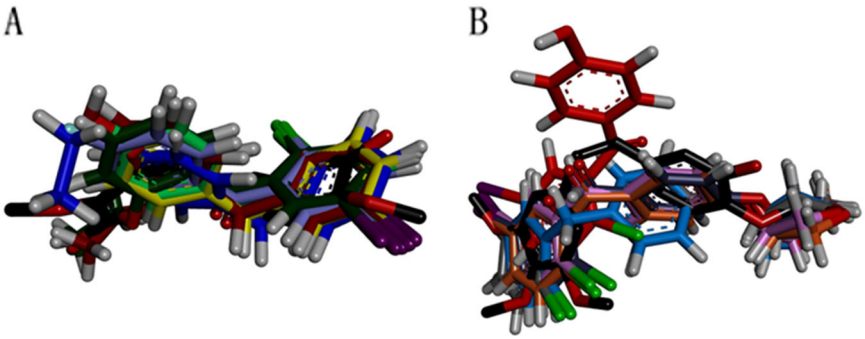

Fig. 2 superimposition of HPAs onto CA-4(carbon atoms of CA-4 show black; iodine atoms show purple; chlorine atoms show green). A mode HT (compounds **1a**, **1c**, **2a**, **2b**, **2c**, and **2f**), B mode HH (compounds **1b**, **1d**, **1e**, **1f**, **2d**, and **2e**)

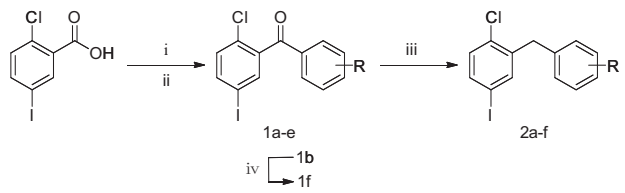

Scheme 2 Reagents and conditions: (i) $(COCl)_2$, ArH, DMF(cat.), CH_2Cl_2, 4 h, rt; (ii) $AlCl_3$, CH_2Cl_2, 3–5 h, 10–20 °C; (iii) $BF_3{\cdot}OEt_2$, Et_3SiH, CH_2Cl_2, 3–8 h, 0–20 °C; (iv) BBr_3, CH_2Cl_2, −20 °C- rt

Anticancer activity

All the HPAs **1a**–**1f** and **2a**–**2f** were tested for anticancer activity against liver cancer cell line Huh-7 (Wei et al. 2016) and lung cancer cell line A549 (Acharya et al. 2011) as microtubule destabilizing agent. The resulting data (Table 3) show that all the tested compounds had generally considerable activity against human liver cancer Huh-7 cells with 27.91–77.61% inhibition and human lung cancer A549 cell line with 25.24–78.08% inhibition at 10 μM concentration, respectively. **1b** (R = *p*-OEt) and **1f** (R = *p*-OH) were acted as active agents against human liver cancer Huh-7 cells with IC_{50} value of 5.53 and 5.47 μM, respectively.

Combined with antitumor activity and docking patterns, it can be concluded that the antitumor activity of the compound with mode HT is not so good. This may due to the halogenated benzene ring failed to interaction with the pocket shaped by residues CYS241, LEU242, ALA250,

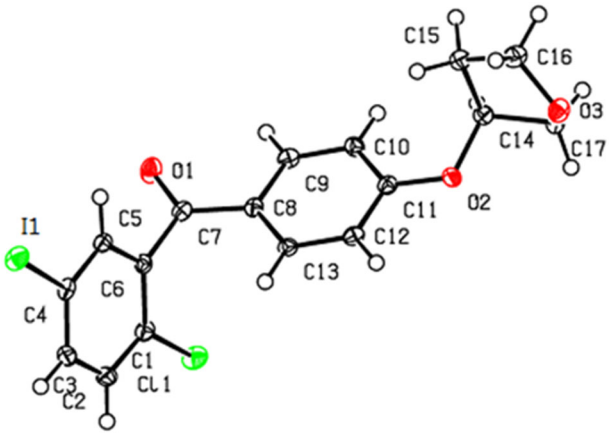

Fig. 3 The X-ray crystal structure of product **1d** with the atom-numbering and displacement ellipsoids are drawn at 50% probability level

Table 3 Anticancer activities of HPAs[a]

Compound	Inhibition (%)	
	Huh-7	A549
1a	32.05	27.80
1b	68.97[b]	73.30
1c	51.27	55.50
1d	36.46	31.44
1e	36.39	36.15
1f	77.61[c]	78.08
2a	31.40	31.22
2b	42.05	32.87
2c	44.85	33.09
2d	27.91	29.95
2e	28.96	25.24
2f	33.82	27.52
Vincristine	83.03	82.67

[a]Huh-7 and A549 cells were treated with 10 μmol/L compounds **1a**–**1f** and **2a**–**2f** for 48 h

[b]IC_{50} value of 5.53 μM against human liver cancer Huh-7 cells

[c]IC_{50} value of 5.47 μM against human liver cancer Huh-7 cells

LEU255, and ALA354 by alkyl hydrophobic. The pocket interacts with the A ring of CA-4 by alkyl hydrophobic as well.

When the substituent of R is p-tetrahydrofuran-3-oxyl, the virtual screening results of compound **1d**, **1e**, **2d**, and **2e** are outstanding in its class (ΔG (kcal/mol) = −7.21 to −7.52, Ki (μM) = 5.15 to 3.08). It may be due to their insertation in the pocket with mode HH and more hydrogen bonds formed between the tetrahydrofuran ring and amino acid residues. However, the tetrahydrofuran ring has stretched to the edge of the pocket shaped by residues THR179, ALA180, VAL181, MET259, ALA316, and ASN349

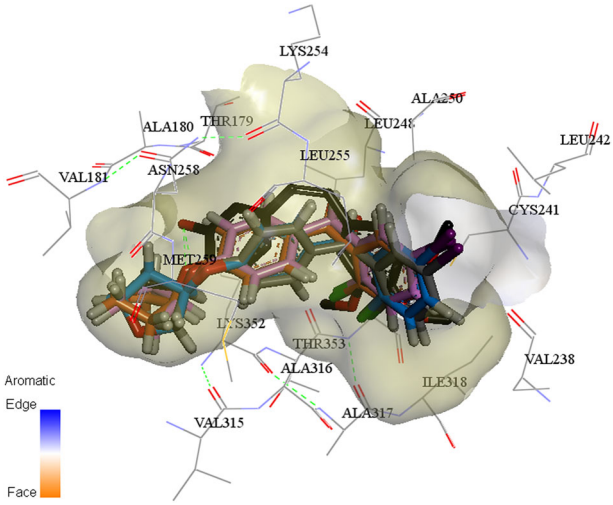

Fig. 4 Stacked plots of compound **1d**, **1e**, **2d**, and **2e** with CA-4 in colchicine site of tubulin

(Fig. 4). The steric hindrance may be result in its lack of anticancer activity.

The compound **1b** and **1f** show good anticancer activity. Both the *p*-OH or *p*-OEt group of the non-halogenated benzene ring can form hydrogen bonds with amino acid residues, which contribute to the increased activity. Compared with their reduction products (**2b** and **2f**), carbonyl group makes their dominant conception to interact with colchicine site via mode HH, which make them less active.

Concerning **1a**–**1f** and **2a**–**2f**, it was also found that both docking results and anticancer activity were tending to the carbonyl (Y = CO) between diaryl rings is favor.

Conclusion

In conclusion, the results of docking study of HPAs were proved that they are better microtubule destabilizing agent than CA-4 or Phenstatin. The docking and anticancer activitie results demonstrate that mode HH is a dominant conformation than mode HT that provides a path for future design of new microtubule destabilizing agent. The HPAs were synthesized within three-step reaction with appropriate yield. All the products were characterized by ^{1}H NMR and ^{13}C NMR spectral analysis, especially the stereochemical structures of pruduct **1d** was also confirmed by single crystal X-ray diffraction crystallographic analysis. The anticancer activities of HPAs showed that all the tested compounds had generally considerable activities against human cancer Huh-7 and A549 cell lines with 27.91–77.61% and 25.24–78.08% inhibition at 10 μM concentration, respectively. In particular, the **1b** and **1f** were found to be potent inhibitors against Huh-7 cancer cell line with IC_{50} value of 5.53 and 5.47 μM, respectively.

Acknowledgements We are grateful for the financial support from 2015 Beijing Natural Science Foundation (No. KZ201510005007) and thank professor Honggen Wang in Nankai University for single crystal X-ray diffraction technical assistance.

Compliance with ethical standards

Conflict of interest The authors declare that they have no conflict of interest.

Publisher's note: Springer Nature remains neutral with regard to jurisdictional claims in published maps and institutional affiliations.

References

Acharya BR, Bhattacharyya S, Choudhury D, Chakrabarti G (2011) The microtubule depolymerizing agent naphthazarin induces both apoptosis and autophagy in A549 lung cancer cells. Apoptosis 16:924–939

Álvarez C, Álvarez R, Corchete P, Pérez-Melero C, Peláez R, Medarde M (2010) Exploring the effect of 2,3,4-trimethoxy-phenyl moiety as a component of indolephenstatins. Eur J Med Chem 45:588–597

Beale TM, Myers RM, Shearman JW, Charnock-Jones DS, Brenton JD, Gergely FV, Ley SV (2010) Antivascular and anticancer activity of dihalogenated A-ring analogues of combretastatin A-4. Med Chem Commun 1:202–208

Gaspari R, Prota AE, Bargsten K, Cavalli A, Steinmetz MO (2017) Structural basis of cis-and trans-combretastatin binding to tubulin. Chem 2:102–113

Gaukroger K, Hadfield JA, Lawrence NJ, Nolan S, McGown AT (2003) Structural requirements for the interaction of combretastatins with tubulin: how important is the trimethoxy unit? Org Biomol Chem 1:3033–3037

Kingston DG (2009) Tubulin-interactive natural products as anticancer agents. J Nat Prod 72:507–515

Li M, Tian YS (2016) Progress in synthesis and anti-tumor activities of combretastatin A4 derivatives. J Pharm Res 35:283–289

Lin CM, Ho HH, Pettit GR, Hamel E (1989) Antimitotic natural products combretastatin A-4 and combretastatin A-2: studies on the mechanism of their inhibition of the binding of colchicine to tubulin. Biochemistry 28:6984–6991

Marrelli M, Conforti FA, Statti G, Cachet X, Michel S, Tillequin F, Menichini F (2011) Biological potential and structure-activity relationships of most recently developed vascular disrupting agents: an overview of new derivatives of natural combretastatin A-4. Curr Med Chem 18:3035–3081

Nguyen TL, McGrath C, Hermone AR, Burnett JC, Zaharevitz DW, Day BW, Wipf P, Hamel E, Gussio R (2005) A common pharmacophore for a diverse set of colchicine site inhibitors using a structure-based approach. J Med Chem 48:6107–6116

Pettit GR, Anderson CR, Herald DL, Jung MK, Lee DJ, Hamel E, Pettit RK (2003) Antineoplastic agents. 487. Synthesis and biological evaluation of the antineoplastic agent 3,4-methylenedioxy-5,4'-dimethoxy-3'-amino-Z-stilbene and derived amino acid amides. J Med Chem 46:525–531

Pettit GR, Cragg GM, Herald DL, Schmidt JM, Lohavanijaya P (1982) Isolation and structure of combretastatin. Can J Chem 60:1374–1376

Pettit GR, Grealish MP, Herald DL, Boyd MR, Hamel E, Pettit RK (2000) Synthesis of the cancer cell growth inhibitor hydroxyphenstatin and its sodium diphosphate prodrug. J Med Chem 43:2731–2737

Pettit GR, Minardi MD, Rosenberg HJ, Hamel E, Bibby MC, Martin SW, Jung MK, Pettit RK, Cuthbertson TJ, Chapuis JC (2005) Antineoplastic agents. 509: synthesis of fluorcombstatin phosphate and related 3-halostilbenes. J Nat Prod 68: 1450–1458

Pettit GR, Toki B, Herald DL, Verdier-Pinard P, Boyd MR, Hamel E, Pettit RK (1998) Synthesis of phenstatin phosphate1a. J Med Chem 41:1688–1695

Singh R, Kaur H (2009) Advances in synthetic approaches for the preparation of combretastatin-based anti-cancer agents. Synthesis 2009:2471–2491

Titov IY, Sagamanova IK, Gritsenko RT, Karmanova IB, Atamanenko OP, Semenova MN, Semenov VV (2011) Application of plant allylpolyalkoxybenzenes in synthesis of antimitotic phenstatin analogues. Bioorg Med Chem Lett 21:1578–1581

Wang XJ, Zhang L, Byrne D, Nummy L, Weber D, Krishnamurthy D, Yee N, Senanayake CH (2014) Efficient synthesis of empagliflozin, an inhibitor of SGLT-2, utilizing an $AlCl_3$-promoted silane reduction of a β-glycopyranoside. Org Lett 16:4090–4093

Wei RJ, Lin SS, Wu WR, Chen LR, Li CF, Chen HD, Chou CT, Chen YC, Liang SS, Chien ST (2016) A microtubule inhibitor, ABT-751, induces autophagy and delays apoptosis in Huh-7 cells. Toxicol Appl Pharm 311:88–98